# Magneto-Optic Rotations in a terbium gallium garnet crystal

Hasan Ahmed
Roll no: 2021-10-0306
LUMS School of Science and Engineering

Monday, December, 23, 2019

## 1 Abstract

We demonstrate magnetically induced birefringence in a, otherwise optically inactive, dispersive medium. Using a 405nm linearly polarized laser and measurements on a lock-in amplifier we were able to measure the verdet constant of a Terbium Gallium Garnet (TGG) crystal.

## 2 Introduction

Terbium Gallium Garnet is an optically inactive (non-chiral) dispersive medium. In other words, the medium is frequency dependant and so electromagnetic waves of different frequencies travel at different velocities but it cannot differentiate between right-circularly polarized and left-circularly polarized light. Chirality (or circular birefringece) can be induced using magnetisation, this phenomenon is known as the Faraday Effect.

The verdet constant is a measurement used to quantify the extent of this induction is a function of the wavelength of light, temperature and refractive index of the material:

$$V = V(\lambda, T, n). \tag{1}$$

The verdet constant is the rotation per unit path length per unit applied magnetic field:

$$\theta = V \int_0^d B(z)\ dz, \tag{2}$$

where $d$ is the length of the medium.

These techniques finds uses in anything from measuring the speed of artillery projectiles [1] to performing diagnostics on blood samples [2].

A schematic of the experimental setup is given below [3]:

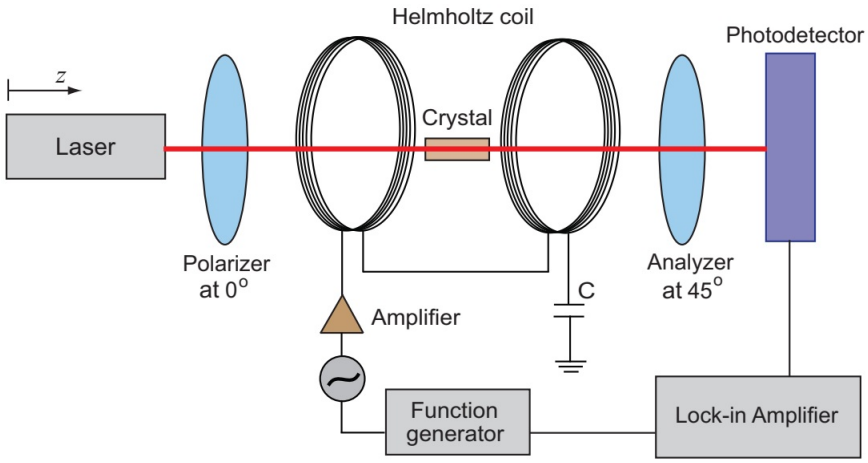


Figure 1: Setup to measure verdet constant of the TGG crystal

# 3 Theoretical primer I

## 3.1 Birefringence

In a nutshell, birefringence is the property of a medium to assign a different refractive index to RCP and LCP light.

Using Jones Calculus, one can show that linearly polarized light is simply the sum of RCP and LCP light of equal frequency and amplitude since,

$$\widetilde{E}_{LCP} = a \begin{bmatrix} 1 \\ i \end{bmatrix} \; and \; \widetilde{E}_{RCP} = b \begin{bmatrix} 1 \\ -i \end{bmatrix}. \tag{3}$$

Add these together gives us:

$$\widetilde{E} = \widetilde{E}_{LCP} + \widetilde{E}_{RCP} = \begin{bmatrix} a+b \\ i(a-b) \end{bmatrix} = \begin{bmatrix} \widetilde{E}_{0x} \\ \widetilde{E}_{0y} \end{bmatrix}. \tag{4}$$

Here, $(a+b)$ and $(a-b)$ are the major and minor axes of an ellipse respectively.

$$\therefore \; \widetilde{E}_{0x} = (a+b)e^{i(kz-wt)} \text{ and } \widetilde{E}_{0y} = (a-b)e^{i(kz-wt+\frac{\pi}{2})}.$$

Taking the real part of these components i.e.

$\vec{E_x}(z,t) = E_{0x}cos(kz - wt)$ and $\vec{E_y}(z,t) = E_{0y}sin(kz - wt)$,

one can see that these lead to linearly polarized light with said components in some direction $\hat{r}$.

Now that we have established that a linearly polarized light is simply the sum of RCP and LCP, we can hypothesize that a Birefrengent material change the orientation of the linearly polarized light since the RCP and LCP component will have different refractive indices and therefore a different rate of rotation when passing through the medium. This asymmetry is better realised in a diagram [3], see Figure (2).

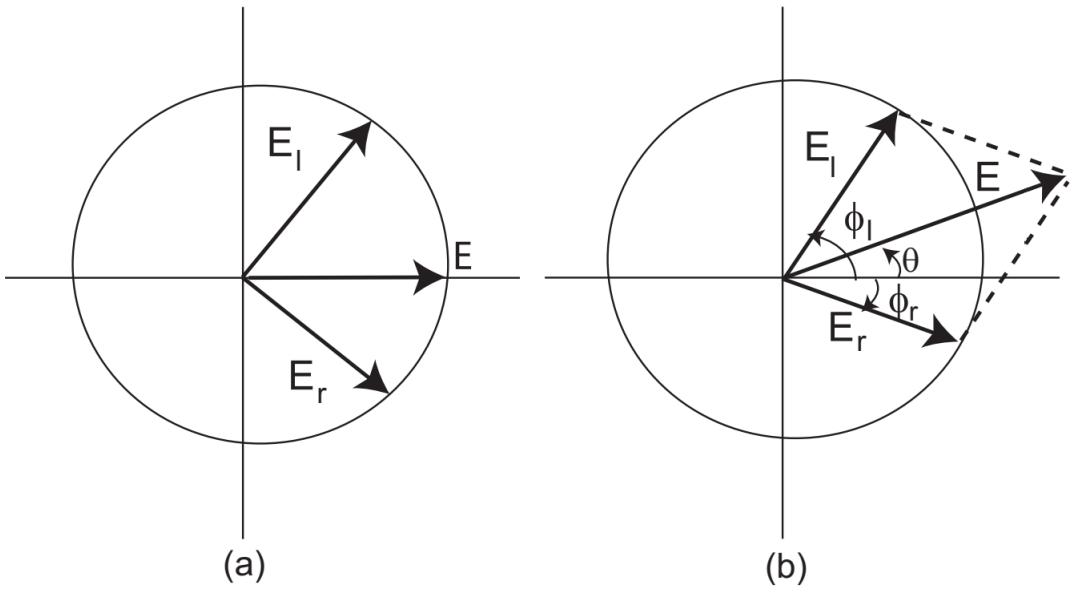


Figure 2: (a) shows the decomposition of linearly polarized light into RCP and LCP. (b) shows the phase difference that is achieved between the RCP and LCP component after passing through the medium, where clearly $\phi_l \neq \phi_r$ and so the resultant has rotated by $\theta$.

## 3.2 Faraday Rotation

Next, we will see how Birefringence can be induced in a material, via the introduction of a magnetic field, $\vec{B}$, that is optically inactive. To understand this, must investigate the material more closely i.e. at the atomic level. A simplified model of an atom will suffice, which is just a nucleus and electrons orbiting around it at radius, $|r|$. The electrons have some magnetic moment, $\vec{\mu_e}$, and an applied magnetic field will generate a torque, $\vec{\tau}$. This will coerce the electron's plane of rotation to precess as shown in the diagram [3] below:

We shall denote the frequency of this precession as, $\nu_L$, the Larmor frequency and the vacuum frequency of the light entering the medium as $\nu$. Now, since the angular momentum vector points such that the precession is either clockwise or

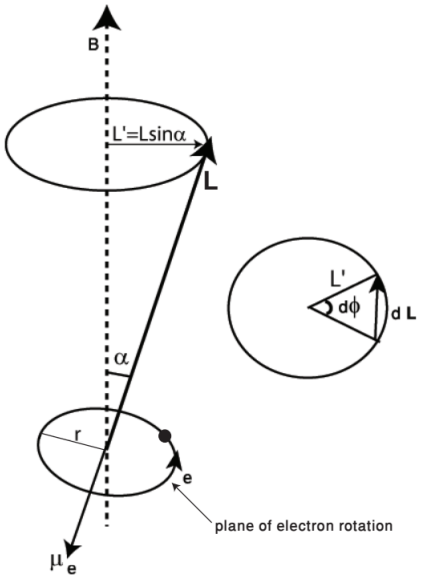


Figure 3: Precession of the plane of rotation of the electron due to applied magnetic field.

anticlockwise, we can say that the LCP light has a frequency of $\nu + \nu_L$ (in the direction of the angular momentum) and the RCP light has $\nu - \nu_L$.

If the medium is dispersive, then it can differentiate between the two frequencies by *allotting* different refractive indices to the components just like a natively birefrengent material.

# 4 Working Principle of a Lock-In Amplifier

Since the Lock-In is an integral part of the experiment and may be unfamiliar to an undergraduate student, we present a brief introduction for it.

The lock-in is a device that allows for measurement of the phase and amplitude of an oscillating signal that would otherwise be lost in the noise using information about its frequency dependence.

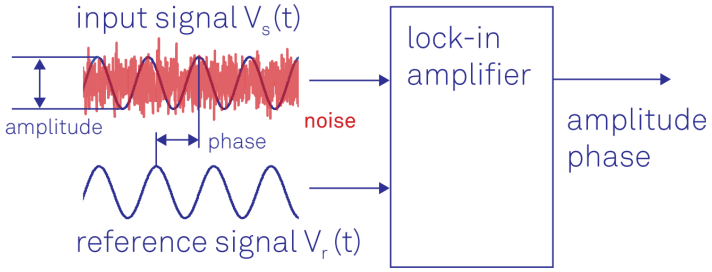


Figure 4: The lock-in can make use of a defined reference signal to measure signals buried in the noise [4]

The lock-in takes in the input signal, along with the noise, and the reference signal and passes them through a mixer which is essentially the same as multiplying the two signals.

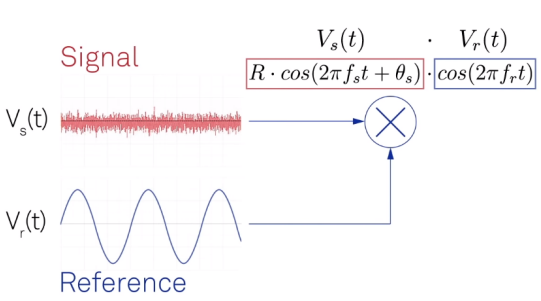


(a) Signals in the time domain [4].

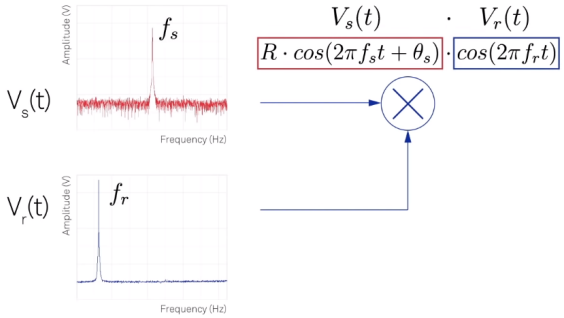


(b) Signals in the frequency domain [4].

Here $f_s$ is the signal frequency and $f_r$ is the reference frequency. $\theta_s$ is the phase difference between the signal and reference frequency but for most experiments we use the reference frequency as the the input signal for our experiment as well and so this $\theta_s$ is eliminated and the multiplication of the two signals simply gives us two new frequencies, one at the difference and one at the sum of the two frequencies (signal and reference).

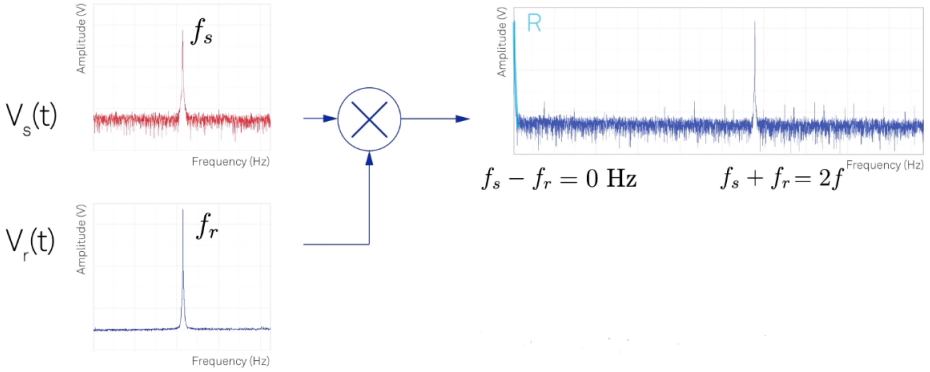


Figure 6: We see frequencies at the 0 Hz mark(or DC component) and the $2f$ mark [4].

To measure the DC component of the incoming signal from the mixer we introduce a low pass filter. A low pass filter will allow only a certain range of frequencies and has an upper bound dictated by a post time constant,$\tau_p$. Past the cut-off frequency, $f_c$, the signal is attenuated by half and is proportional to $\tau_p$:

$$f_c \propto \frac{1}{\tau_p} \tag{5}$$

The bandwidth refers to range of frequencies below $f_c$ and it is worth mentioning the trade-offs between a wide and narrow bandwidth.

A wider bandwidth can allow the $2f$ component to leak in, and allow more noise in enter the measurement thus a lower signal to noise ratio but allows for faster readings, and vise versa for a narrow bandwidth.

# 5 Experimental Preliminaries and results

## 5.1 Finding the resonant frequency of the Helmholtz coil

Since we are using an RLC circuit, there must exist a resonant frequency for circuit[1], this will aid us in creating a strong uniform magnetic field to apply to the TGG crystal when calculating the verdet constant.

The setup was assembled as such:

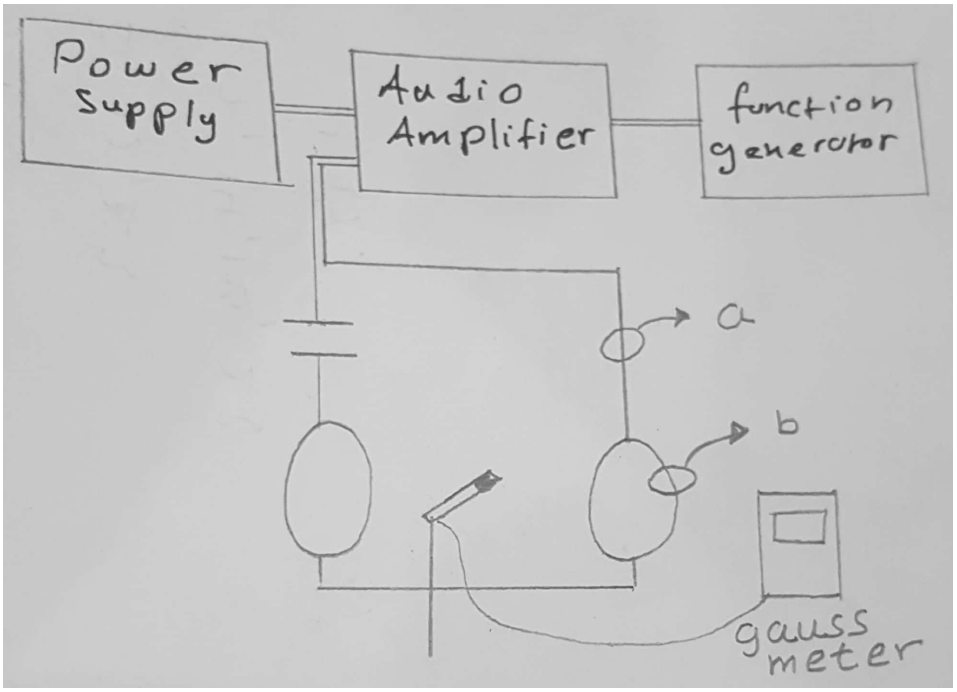


Figure 7: Setup for measurement of the resonant frequency of the Helmholtz coils and relationship between measured magnetic field and current in coils

For this section, the gauss meter was omitted. The function was stepped up in frequency and measurement of current taken at two points, point **a** and point **b**. point b had the distinct advantage of greater sensitivity since the coils of the Helmholtz served as a multiplier to the value obtained on the clamp meter.

The table below (1) shows our readings for different frequencies on the function generator and clamp meter connected at point **b**[2].

[1]You can also hear a ringing sound at this frequency of twice the frequency, this may be due to the magnetic field being induced between the Helmholtz coils causing them to vibrate but at twice the frequency since the forces on Helmholtz change direction twice for every cycle of current.

[2]Since a rough measurement indicated the likely frequency at which the circuit would resonant the increments of the frequencies were spaced closer as we approached the resonant frequency.

| Frequency (Hz) | Current (A) |
|---|---|
| 100 | 8.4 |
| 150 | 12.2 |
| 200 | 15.2 |
| 250 | 18.8 |
| 300 | 22.7 |
| 350 | 27.6 |
| 400 | 33.5 |
| 450 | 40.8 |
| 500 | 50.3 |
| 550 | 66.3 |
| 600 | 82.1 |
| 650 | 112.5 |
| 700 | 168.9 |
| 750 | 307 |
| 770 | 437 |
| 790 | 680 |
| **810** | **926** |
| 830 | 704 |

| Frequency (Hz) | Current (A) |
|---|---|
| 850 | 470 |
| 870 | 339 |
| 890 | 258 |
| 910 | 209 |
| 930 | 175 |
| 950 | 151 |
| 1000 | 114.9 |
| 1050 | 90.7 |
| 1100 | 77.3 |
| 1150 | 66.5 |
| 1200 | 59.1 |
| 1250 | 53.1 |
| 1300 | 48.0 |
| 1350 | 43.9 |
| 1400 | 40.6 |
| 1450 | 37.7 |
| 1500 | 35.0 |
| 1550 | 33.4 |
| 1600 | 31.5 |

Table 1: Relationship between frequency of function generator and current in Helmholtz coils. We see a maximum at 810 Hz.

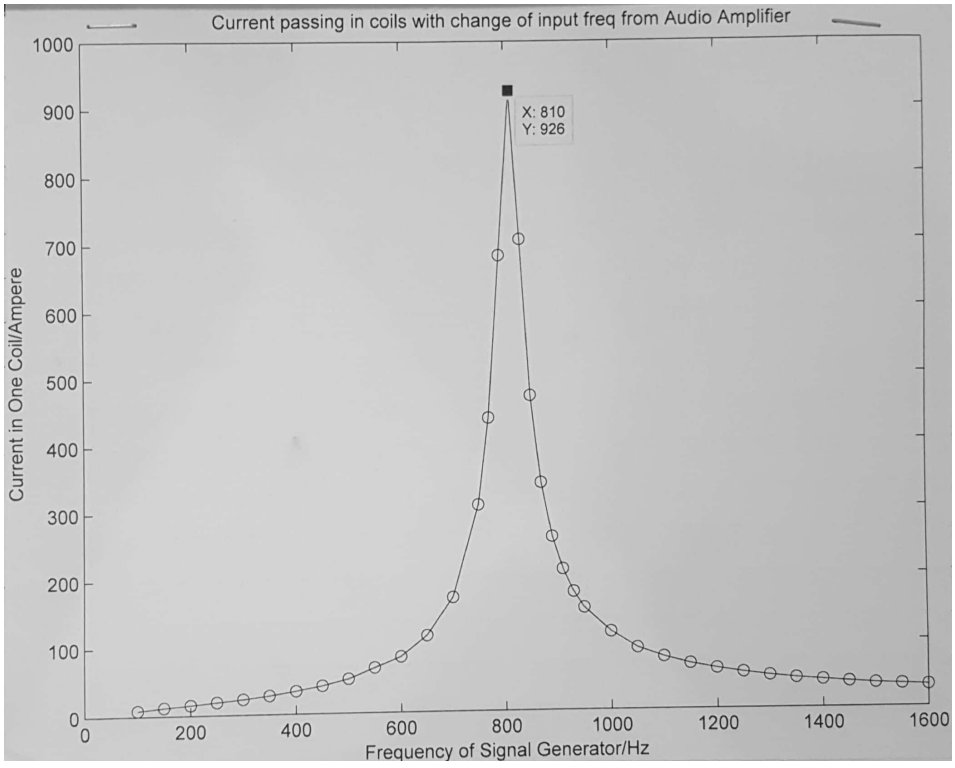


Figure 8: Resonant frequency of the circuit around 810 Hz for our particular circuit.

## 5.2 Measuring the magnetic field produced by the coils

Next, we added the gauss meter to our setup, aided by a clampstand because the probe was very sensitive to minute shaking of the hand. What we tried doing here is to find a calibration line between the magnetic field produced at the region where we will eventually place the TGG crystal and the current in the wire at point **a**. This serves two purposes, one being convenience since it is simply easier to take measurements with a clampmeter rather than a probe that may not remain perfectly stationary throughout the experiment and second, that we cannot place the probe *at* the location of the TGG crystal during the experiment so we are inviting a systematic error[3].

We set the function generator at the resonating frequency[4] and increased the amplitude of the output voltage of the function generator to tabulate the following:

| Output Voltage (V) | Current (A) | Magnetic Field (G) |
|---|---|---|
| 0.1 | 0.2 | 9.7 |
| 0.2 | 0.6 | 19.8 |
| 0.3 | 1.0 | 29.8 |
| 0.4 | 1.3 | 39.7 |
| 0.5 | 1.7 | 49.7 |
| 0.6 | 2.1 | 59.8 |
| 0.7 | 2.5 | 69.6 |
| 0.8 | 2.9 | 79.5 |
| 0.9 | 3.2 | 89.1 |
| 1.0 | 3.6 | 98.1 |
| 1.1 | 3.9 | 106.8 |
| 1.2 | 4.2 | 115.8 |
| 1.3 | 4.6 | 124.1 |
| 1.4 | 4.8 | 130.1 |
| 1.5 | 4.9 | 133.6 |
| 1.6 | 5.0 | 135.5 |

We can graph the above table to give us a calibration line. The best fitted line had a calibration[5] given by:

$$|\mathbf{B}|(G) = 26.23\ \mathbf{I}(A) + 4.439 \tag{6}$$

The additional value of 4.439 may be due to some background reading or experimental inaccuracy. The data is graphed below.

[3]For our purposes this difference was negligible and thus the calibration can be ignored all together. The reader may choose to skip ahead.

[4]To maximize the magnetic field and to ensure consistency in our experiment.

[5]For our setup

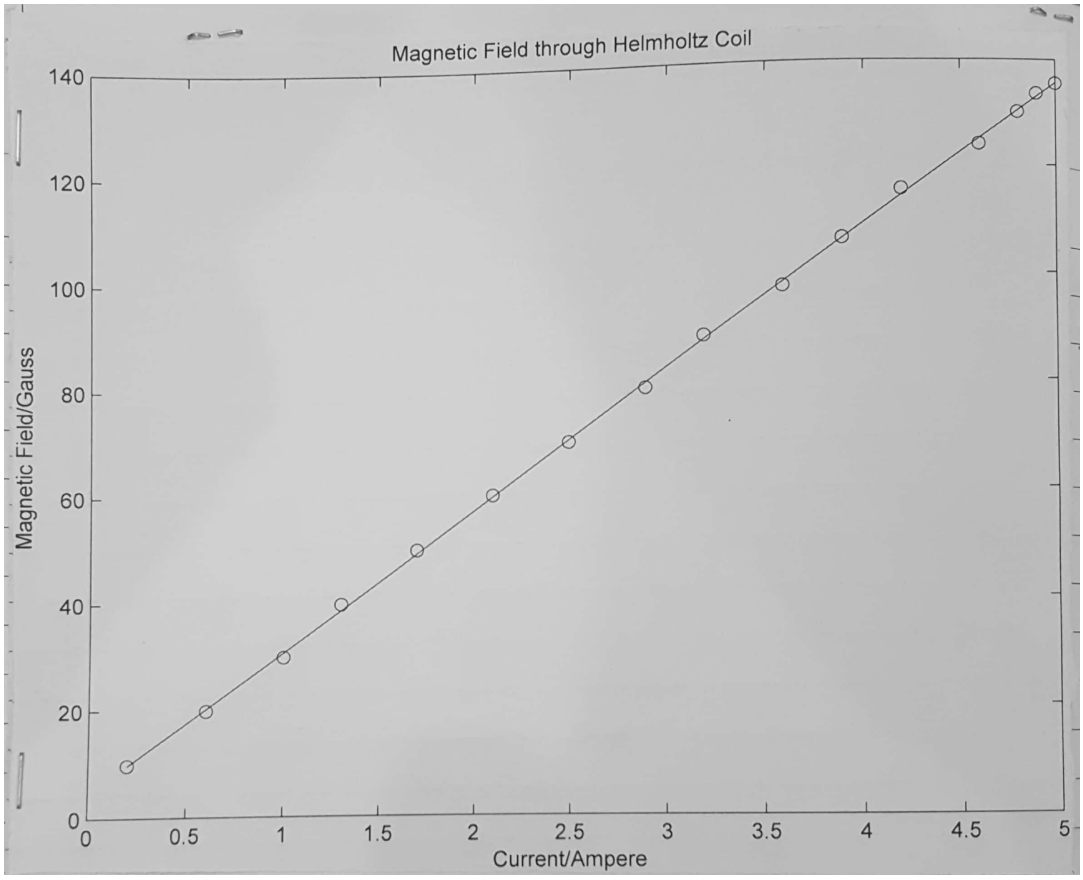


Figure 9: Calibration line that can be help us use magnetic field at the center and current in the circuit interchangeably for convenience.

# 6 Theoretical Primer II

## 6.1 Malus' Law

Before we proceed to the final stage of the experiment, an essential detour is needed. The attentive reader may have noticed the fact that in Figure (1) the "Analyzer" is at 45° with respect to the polarizer. We will present the crux of the argument as Malus' Law. We hope that the reader can digest this without experimental proof since this is not the purpose of the demonstration but is important nonetheless. The law states that the intensity of a plane polarized light, $I_0$, after passing through a rotatable polarizer varies as the square of the cosine of the relative angle, $\theta$. In other words:

$$I = I_0 cos^2(\theta) \tag{7}$$

The diagram below illustrates this.

We shall use this law to help us find the maximum change of intensity with respect to the angle that is rotated by the sample.

A slight complication in our case is the introduction of a sample that through

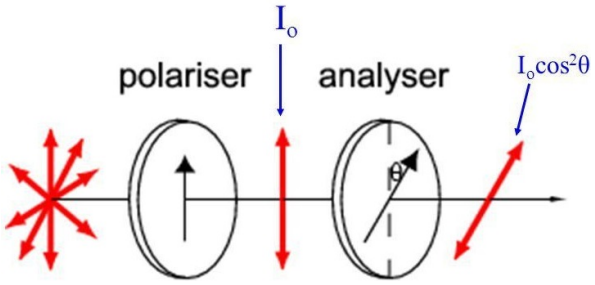


Figure 10: Variation of the output intensity as a function of the relative angle $\theta$ is given by Malus' Law [5]

induced birefrengence rotates the plane polarized beam of light before the analyzer. This only introduces a modifier to the Malus' law to:

$$I = I_0 cos^2(\theta - \phi). \tag{8}$$

Here, $\phi$ is the angle by which the sample rotates the plane of polarization.

## 6.2 Optimizing the analyzer angle

To maximize change in intensity, we must set the second derivative with respect to $\theta$ to 0, therefore, we have:

$$\frac{dI}{d\theta} = 2I_0 cos(\theta - \phi) sin(\theta - \phi) \tag{9}$$

$$= I_0 sin(2(\theta - \phi)) \tag{10}$$

and,

$$\frac{d^2 I}{d\theta^2} = 2I_0 cos(2(\theta - \phi)), \tag{11}$$

and setting this to 0 implies:

$$\theta - \phi = 45°. \tag{12}$$

Now, since $\phi << \theta$, we can see that setting the analyzer at 45° ($\theta = 45°$) gives us the maximum change in intensity.

We can use this approximation in equation (8) to give:

$$I = \frac{I_0}{2}[1 + cos(2(\theta - \phi))] \tag{13}$$

$$= \frac{I_0}{2}[1 + cos(2\theta)cos(2\phi) + sin(2\theta)sin(2\phi)] \tag{14}$$

$$I \approx \frac{I_0}{2}[1 + 2\phi] \tag{15}$$

### 6.3 Converting light intensities into photocurrents

Take note that since our magnetic field for Faraday rotations is oscillatory, then the angle by which the sample rotates the plane polarized light is proportional to the magnetic field:

$$B \propto \phi \tag{16}$$

$$B = B_0 sin(\omega t) \tag{17}$$

$$\phi = \phi_0 sin(\omega t) \tag{18}$$

$\therefore$ I $\approx \frac{I_0}{2}[1 + 2\phi_0 sin(\omega t)]$.

In our experiment, we will be using a photodiode to convert the intensity of light into current. We can see that the intensity has a stationary DC component and an oscillatory AC component,

$\therefore$ i $= \mathrm{i}_{dc} + i_{ac}$, where $i_{dc} = I_0/2$ and $i_{ac} = I_0\theta_0 sin(\omega t)$. We will be measuring this using a lock-in, which gives us an rms value for $i_{ac}$ instead.

$\therefore$ $\mathrm{i}_{rms} = I_0\theta_0/\sqrt{2}$.

It is easy to see now that the ratio of $i_{rms}$ and $i_{dc}$ gives us $\theta_0$ which is just $\theta_{rms}$.

We can now make use of equation (2), for a uniform magnetic field throughout the sample this reduces to:

$$\theta_{rms} = V B_{rms} d \tag{19}$$

It is reasonable to see why the ratio of the two currents gives us $\theta_{rms}$, since the $i_{dc}$ component is simply the intensity when the magnetic field is turned off and vise versa for $i_{ac}$. So in essence we are measuring the factor by which the plane polarized light rotates with and without the magnetic field on[6].

We now have all the tools needed for the final result.

## 7 Experimental Procedure

We setup the experiment as shown[7] in Figure (1), being careful to keep the photodiode as far as possible from the Helmholtz coils due to its sensitivity to magnetic fields.

[6] Of course, without the magnetic field on this would mean no rotation at all since our sample does not show birefringent properties

[7] A slight modification needed to our arrangement was to add an I/V converter for the lock-in to show readings in voltage instead of ampere but this only introduced an multiplication factor

Now, with the laser on, sample placed and magnetic field off, we measured the current output of the photodetector to be $\boxed{3.55\text{e-}8\ A}$, which is $i_{dc}$.

Next we set the function generator at the resonating frequency, and adjusted the amplitude to produce a magnetic field of 10.0G at the location of the TGG crystal[8].

The amplitude of the audio amplifier was adjusted to incrementally increase the magnetic field and the values on the lock-in were tabulated, these correspond to the values of $i_{rms}$.

Using the relationship between the $\theta_{rms}$ and the components of current and equation (19), we have:

$$\frac{i_{rms}}{\sqrt{2}i_{dc}} = VB_{rms}d \tag{20}$$

Our measurement values are given below.

| $B_{rms}(G)$ | $i_{rms}$ (nA) |
|---|---|
| 10.6 | 0.13 |
| 20.8 | 0.26 |
| 30.5 | 0.37 |
| 40.0 | 0.49 |
| 51.4 | 0.63 |

| $B_{rms}(G)$ | $i_{rms}$ (nA) |
|---|---|
| 62.6 | 0.76 |
| 70.4 | 0.86 |
| 81.4 | 0.98 |
| 91.1 | 1.10 |
| 101.3 | 1.23 |

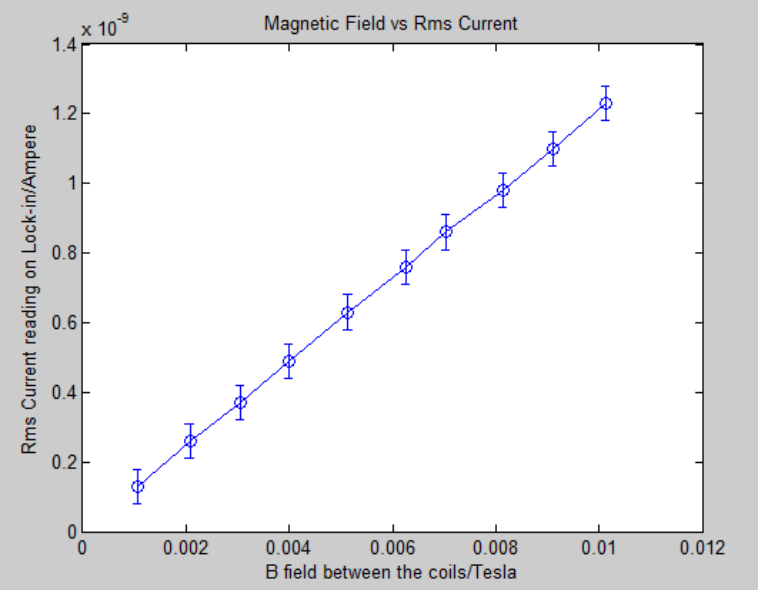


Figure 11: Graph showing relationship between $i_{rms}$ and the magnetic field at the location of the sample.

We can use the gradient of the graph above and our equation (20) to conclude that the for our sample[9], the verdet constant is $\boxed{240 \pm 10\ \mathrm{T}^{-1}m^{-1}}$.

[8]from this point on, no adjustments to the function generator were made since we need to keep the reference being used the same

[9]The TGG crystal we used had $d = 1$ cm

# 8 Conclusion

Using phase sensitive detection, we can quantitatively measure macroscopic phenomenon that would otherwise be undetectable, forever obscured by noise. In the demonstration above, we are able to measure currents in the nano-scale, we can push this even further by employing more carefully isolated experiments. As we approach a quantum age, more subtle perturbations in our previous assumptions can be knocked down one by one or more grander experiments such as vibrations due to gravitational waves from distant merging black holes.

As for the birefringence of a material, we have referenced possible uses of such materials in the introduction. And being able to induce these properties onto a wide range of materials opens up another realm of possibilities.

Take note, the value we obtained for the verdet constant is simply from the fundamental frequency reading on the lock-in and taking reading using the higher harmonics can get you closer to the true value and therefore a more accurate model for the Faraday rotations in the TGG crystal.

# References


[1] L. Kristjánsson, "*Some practical applications of the Faraday magneto-optic effect, the Kerr electro-optic effect, and the Pockels electro-optic effect in the early decades of the 20th century*", Institute of Earth Science ,University of Iceland, (2017).

[2] Jijo J. Vallooran, "*Lipidic Cubic Phases as a Versatile Platform for the Rapid Detection of Biomarkers, Viruses, Bacteria, and Parasites.*" Advanced Functional Materials, (2015).

[3] S. Anwar, A. Aftab and A. Shaheen "*Phase Sensitive Faraday Rotation*", LUMS School of Science and Engineering, (2016).

[4] Zurich, "*Principles of lock-in detection and the state of the art*, Zurich Instruments, (2016).

[5] Cowen Physics, "*Malus' Law*", https://www.youtube.com/watch?v=utY72MD-Ii4, (2015).